Received: 28 July 2021 | Accepted: 26 August 2021

DOI: 10.1002/mgg3.1809

Molecular Genetics & Genomic Medicine Open Access WILEY

ORIGINAL ARTICLE

Novel variants in *KAT6B* spectrum of disorders expand our knowledge of clinical manifestations and molecular mechanisms

Megan Yabumoto[1,2] | Jessica Kianmahd[3] | Meghna Singh[1,2] | Maria F. Palafox[1,2] | Angela Wei[2] | Kathryn Elliott[2] | Dana H. Goodloe[4] | S. Joy Dean[4] | Catherine Gooch[5] | Brianna K. Murray[6] | Erin Swartz[6] | Samantha A. Schrier Vergano[6] | Meghan C. Towne[7] | Kimberly Nugent[8,9] | Elizabeth R. Roeder[8,9] | Christina Kresge[10] | Beth A. Pletcher[10] | Katheryn Grand[11] | John M. Graham Jr.[11] | Ryan Gates[12] | Natalia Gomez-Ospina[12] | Subhadra Ramanathan[13] | Robin Dawn Clark[13] | Kimberly Glaser[14] | Paul J. Benke[14] | Julie S. Cohen[15,16] | Ali Fatemi[15,16] | Weiyi Mu[17] | Kristin W. Baranano[16] | Jill A. Madden[18,19] | Cynthia S. Gubbels[18] | Timothy W. Yu[18] | Pankaj B. Agrawal[18,19,20] | Mary-Kathryn Chambers[21] | Chanika Phornphutkul[21] | John A. Pugh[22] | Kate A. Tauber[23] | Svetlana Azova[24] | Jessica R. Smith[24] | Anne O'Donnell-Luria[18] | Hannah Medsker[25] | Siddharth Srivastava[25] | Deborah Krakow[1,26] | Daniela N. Schweitzer[3] | Valerie A. Arboleda[1,2]

[1]Department of Human Genetics, David Geffen School of Medicine, UCLA, Los Angeles, California, USA

[2]Department of Pathology and Laboratory Medicine, David Geffen School of Medicine, UCLA, Los Angeles, California, USA

[3]Division of Medical Genetics, Department of Pediatrics, David Geffen School of Medicine, UCLA, Los Angeles, California, USA

[4]Department of Genetics, University of Alabama at Birmingham, Birmingham, Alabama, USA

[5]Department of Pediatrics, Washington University School of Medicine in St. Louis, St. Louis, Missouri, USA

[6]Division of Medical Genetics and Metabolism, Children's Hospital of The King's Daughters, Norfolk, Virginia, USA

[7]Ambry Genetics Corp, Aliso Viejo, California, USA

[8]Department of Pediatrics, Baylor College of Medicine, San Antonio, Texas, USA

[9]Department of Molecular and Human Genetics, Baylor College of Medicine, Houston, Texas, USA

[10]Department of Pediatrics, Division of Clinical Genetics, Rutgers New Jersey Medical School, Newark, New Jersey, USA

[11]Department of Pediatrics, Cedars-Sinai Medical Center, Los Angeles, California, USA

[12]Department of Pediatrics, Division of Medical Genetics, Stanford University, Stanford, California, USA

[13]Department of Pediatrics, Division of Medical Genetics, Loma Linda University Children's Hospital, Loma Linda, California, USA

[14]Division of Genetics, Joe DiMaggio Children's Hospital, Hollywood, Florida, USA

[15]Department of Neurology and Developmental Medicine, Kennedy Krieger Institute, Baltimore, Maryland, USA

[16]Department of Neurology, Johns Hopkins School of Medicine, Baltimore, Maryland, USA

[17]Department of Genetic Medicine, Johns Hopkins School of Medicine, Baltimore, Maryland, USA

[18]Division of Genetics and Genomics, Department of Pediatrics, Boston Children's Hospital, Harvard Medical School, Boston, Massachusetts, USA

[19]The Manton Center for Orphan Disease Research, Boston Children's Hospital, Boston, Massachusetts, USA

[20]Division of Newborn Medicine, Department of Pediatrics, Boston Children's Hospital, Boston, Massachusetts, USA

[21]Division of Human Genetics, Warren Alpert Medical School of Brown University, Hasbro Children's Hospital/Rhode Island Hospital, Providence, Rhode Island, USA

[22]Division of Child Neurology, Department of Neurology, Albany Medical Center, Albany, New York, USA

[23]Division of Neonatology, Department of Pediatrics, Albany Medical Center, Bernard and Millie Duker Children's Hospital, Albany, New York, USA

[24]Division of Endocrinology, Boston Children's Hospital, Harvard Medical School, Boston, Massachusetts, USA

[25]Department of Neurology, Boston Children's Hospital, Harvard Medical School, Boston, Massachusetts, USA

[26]Department of Obstetrics and Gynecology, David Geffen School of Medicine, UCLA, Los Angeles, California, USA

Correspondence
Valerie A. Arboleda, 615 Charles E. Young Drive South, Los Angeles, CA 90095, USA.
Email: varboleda@mednet.ucla.edu

Funding information
NIH DP5OD024579.

Abstract

The phenotypic variability associated with pathogenic variants in *Lysine Acetyltransferase 6B* (*KAT6B*, a.k.a. *MORF*, *MYST4*) results in several interrelated syndromes including Say-Barber-Biesecker-Young-Simpson Syndrome and Genitopatellar Syndrome. Here we present 20 new cases representing 10 novel *KAT6B* variants. These patients exhibit a range of clinical phenotypes including intellectual disability, mobility and language difficulties, craniofacial dysmorphology, and skeletal anomalies. Given the range of features previously described for *KAT6B*-related syndromes, we have identified additional phenotypes including concern for keratoconus, sensitivity to light or noise, recurring infections, and fractures in greater numbers than previously reported. We surveyed clinicians to qualitatively assess the ways families engage with genetic counselors upon diagnosis. We found that 56% (10/18) of individuals receive diagnoses before the age of 2 years (median age = 1.96 years), making it challenging to address future complications with limited accessible information and vast phenotypic severity. We used CRISPR to introduce truncating variants into the *KAT6B* gene in model cell lines and performed chromatin accessibility and transcriptome sequencing to identify key dysregulated pathways. This study expands the clinical spectrum and addresses the challenges to management and genetic counseling for patients with *KAT6B*-related disorders.

KEYWORDS

CRISPR, Genitopatellar syndrome, *KAT6B*-related disorders, phenotypic spectrum, Say-Barber-Biesecker-Young-Simpson syndrome, variable expressivity, rare genetic diagnosis

1 | INTRODUCTION

Lysine Acetyltransferase 6B, or *KAT6B* (MIM# 605880; a.k.a *MORF*, *MYST4*), is a gene that encodes a highly conserved histone acetyltransferase protein. KAT6B belongs to the MSYT family of proteins along with KAT6A, KAT5, and KAT7; members of this family are distinguishable by their highly conserved MYST domain with an acetyl-CoA binding motif and a zinc finger (Champagne et al., 2001; Sapountzi & Cote, 2011) and plays a role in transcription activation through the promotion of H3K23 acetylation upon the interaction of the protein with acylated H3K14 (Klein et al., 2019). The MYST family of proteins function in important cellular processes including chromatin remodeling, gene regulation, protein translation, metabolism, and cellular replication (Avvakumov & Cote, 2007; Voss et al., 2009).

De novo truncating variants in the *KAT6B* gene are associated with two distinct clinical syndromes described by a range of phenotypes: Say-Barber-Biesecker-Young-Simpson syndrome (SBBYSS; MIM# 603736) and Genitopatellar syndrome (GPS; MIM# 606170), with

intermediate phenotypes falling on a spectrum between these two syndromes. Major characteristics of SBBYSS include distinctive craniofacial features such as blepharophimosis, "mask-like" facies, a bulbous nose with a broad nasal bridge, hypotonia, difficulties feeding, abnormally long thumbs and long great toes, intellectual disability, and severe developmental delay (Biesecker, 1991; Cavalcanti, 1989; Clayton-Smith et al., 2011; Ohdo et al., 1986; Say & Barber, 1987; Szakszon et al., 2011). Major features of GPS include skeletal dysplasia, absent or hypoplastic patellae, ambiguous genitalia, anal anomalies, renal issues, agenesis of the corpus callosum with microcephaly, and severe motor and intellectual delay (Campeau et al., 2012; Cormier-Daire et al., 2000; Penttinen et al., 2009). Finally, despite the previous standard of classification into either GPS or SBBYSS, a number of individuals display an intermediate phenotype or a phenotype not otherwise specified (NOS). Individuals receiving intermediate or NOS classifications do not easily subcategorize into either condition because of the presence or absence of major features from either disease (Campeau et al., 2012; Lonardo et al., 2019; Marangi et al., 2018).

To help differentiate between SBBYSS and GPS, pathogenic variants and their locations can partially assist in associating specific genotypes with a clinical phenotype (Vlckova et al., 2015). The majority of SBBYSS individuals have pathogenic variants in the distal part of exon 18 (Szakszon et al., 2013) or more proximal variants in exons 13–17. In contrast, the majority of GPS individuals have pathogenic variants in the distal part of exon 17 and in the proximal part of exon 18 (Lonardo et al., 2019) (Figure 1). Given the emergence of cases with an intermediate phenotype, it has become increasingly common to refer to this group of disorders in relation to their gene name, as "*KAT6B*-related disorders." However, the rapidly evolving landscape and knowledge about the spectrum of *KAT6B*-related disorders may complicate the guidance and prognosis by genetic counselors and medical geneticists who have been historically trained to recognize these syndromes as clinically distinct.

Genetic counseling, an important service intended to assist in understanding an individual's genetic health and related decision-making processes, is often incorporated into obstetrics, pediatric, and clinical genetics care. While genetic counseling processes such as consenting for testing, coordinating testing, and educating about results remain consistent across rare diseases, it is important to recognize the need to tailor resources and address specific concerns an individual and/or their family might have. An understanding of how genetic counseling is incorporated

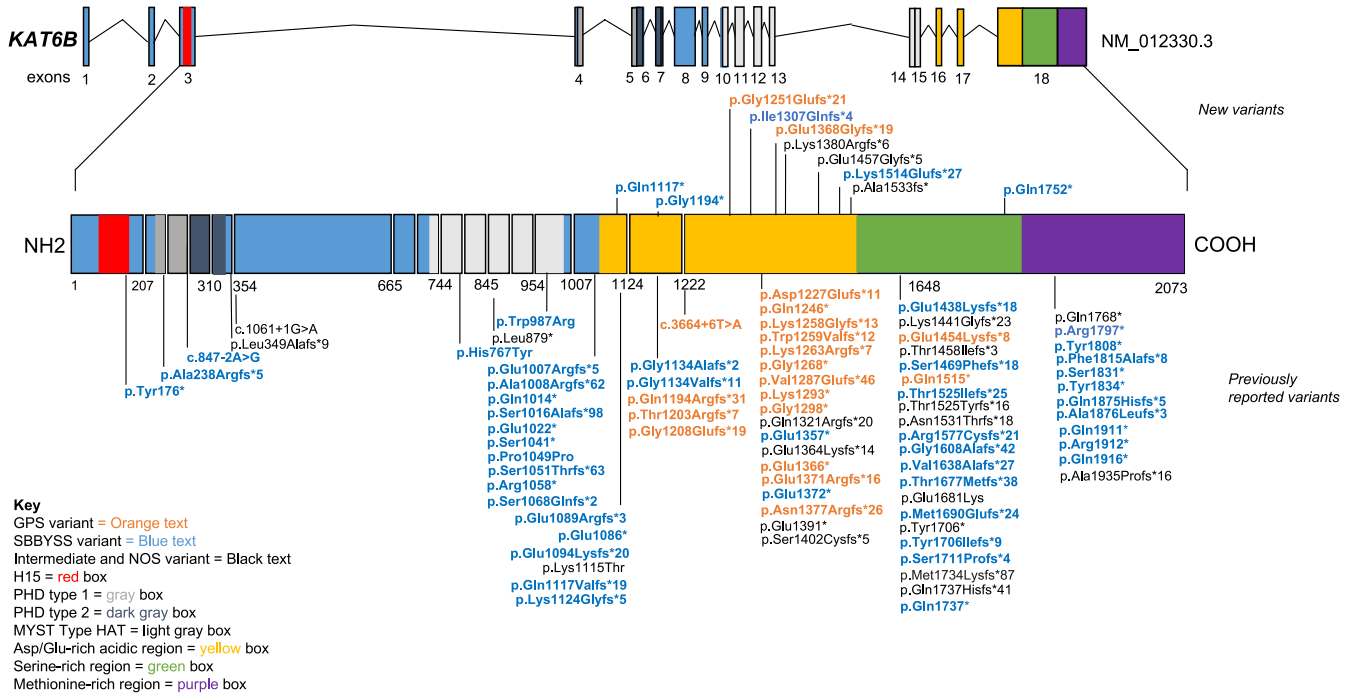

FIGURE 1 Pathogenic variants in *KAT6B*. We added 10 novel variants from our cohort to the list of previously reported variants. The novel pathogenic variants in our cohort are shown above the gene; previously reported variants are displayed below the gene. Genitopatellar (GPS)-related variants are denoted in orange, Say-Barber-Biesecker-Young-Simpson (SBBYS)-related variants are denoted in blue, and intermediate phenotype-related variants are denoted in black. RefSeq ID for *KAT6B* is NM_012330.3. Various protein domains are NEMM domain (AA 1–176), PHD domains (AA 177–360), HAT domain (AA 361–1070), acidic domain (AA 1071–1417), and Ser/Met domain (AA 1418–2073)

into rare disease diagnosis is important in establishing best practices in the management of genomic medicine, particularly for rare diseases with significant phenotypic heterogeneity.

Finally, as gene-centric models of disease have started to take hold, understanding the underlying functional mechanisms that are affected can help us elucidate the effect on molecular and cellular phenotypes that are regulated by KAT6B (Klein et al., 2019; Sheikh et al., 2012). We developed a model of KAT6B truncating variants in a human cell line to explore how these variants result in differential regulation of key transcripts. These types of approaches have been performed in a high throughput manner for tumor suppressor genes like *BRCA1* (Findlay et al., 2018) and *TP53* (Kotler et al., 2018) and can help identify key pathways that are dysregulated by *KAT6B*-related disorders and could be future targets for translational research.

Here, we analyze 20 clinical cases representing a *KAT6B*-related clinical spectrum across three domains: their genotype, phenotype, and experience with genetic counseling resources. Furthermore, we developed an in vitro model of *KAT6B* mutations using CRISPR technology to explore the effect of protein truncation on global transcriptional regulation. Here we demonstrate that the genes that drive core clinical phenotypes are enriched in our in vitro model system. Together, we show that our clinical observations parallel the transcriptional processes in our cell model systems which allow for a further understanding of the mechanisms underlying the *KAT6B*-related clinical spectrum.

2 | MATERIALS AND METHODS

2.1 | Research cohort

We obtained clinical information for a cohort of twenty individuals with pathogenic and likely pathogenic variants in the *KAT6B* gene from 12 different institutions (Figure S1). Of this cohort, 14 individuals were recruited through a call for participation in the case series through the National Society of Genetic Counselors' Pediatrics, Clinical Genetics Special Interest Group, or the Southern California Genetic Counselors Group. Subsequently, six additional individuals were recruited into the study by the colleagues of collaborators.

Phenotypic information was obtained by clinicians and/or genetic counselors with a targeted questionnaire designed to identify a spectrum of clinical features (Table S1). This survey of clinical findings reflects features previously reported to the literature in GPS, SBBYSS, and intermediate cases' reports. A set of questions assessing the role of genetic counselors in the patient's care was appended to the clinical phenotype survey (Table S2). All clinical information was deidentified before the study, as per protocol approved by the Institutional Review Board of the University of California, Los Angeles. Patients and families included in the study provided consent through their treating clinician and additional written consent for the publication of patient photos was obtained.

The variants in *KAT6B* (reference sequence, NM_012330.3) reported by clinicians were identified through whole-exome sequencing or targeted gene panel clinical testing performed at six different laboratories (see Table 1). The original clinical diagnoses provided by clinicians on the questionnaire served to classify individuals into three categories: GPS, SBBYSS, and cases falling within a spectrum between the two subcategories and therefore classified as "intermediate." We then reclassified patients based on the major and minor criteria defined in Zhang et al. (2020), which grouped individuals into *KAT6B* disorder subtypes GPS, SBBYSS, intermediate, and NOS (Table S3). Each individual was evaluated within their category as well as across the cohort to identify major features implicated in *KAT6B*-related disorders.

2.2 | Identification of functional domains

The drawProteins R package was used to make the protein primary structure, with domain and region annotations for KAT6B "Q8WYB5" UniProtKB ID provided by the UniProt API (http://www.uniprot.org/). PTM annotations were downloaded from the PhosphoSitePlus (Hornbeck et al., 2015) and mapped to positions on the primary structure. The conservation metric LIST and the disorder predictors ESpritz (Walsh et al., 2012) and IUPred2a (Mészáros et al., 2018) were sourced from LIST server (Malhis et al., 2019).

2.3 | Cell culture

HEK293T-Cas9-AAVS1 (Genocopeia) cells were grown in DMEM (Gibco™), 10% FBS, and 1% PenStrep at 37℃ in 5% CO_2 incubators. Cell lines were tested for mycoplasma on a monthly basis.

2.4 | CRISPR-mediated introduction of truncating *KAT6B* variants in HEK293T cell line

KAT6B-specific guide RNAs were purchased from Integrated DNA Technologies (see Table S4). Guide RNAs

TABLE 1 Pathogenic variants found in the 20 novel cases included in this report classified using the guidelines in Zhang et al. (2020)

KAT6B related disorder	Individual	Position of variant on NM_012330.3 reference sequence	Predicted effect of mutation	Pathogenicity	Exon	Inheritance	Laboratory	Variant previously observed in other reported case(s)
Genitopatellar Syndrome (GPS)	K6B_1	c.3750delA, p.Gly1251Glufs*21	Frameshift	P	18	de novo	GeneDx	
	K6B_2	c.3769_3772delTCTA, p.Lys1258Glyfs*13	Frameshift	P	18	de novo	Prevention Genetics	Campeau et al. (2012), Simpson et al. (2012), Gannon et al. (2015), Zhang et al. (2020)
	K6B_3	c.3769_3772delTCTA, p.Lys1258Glyfs*13	Frameshift	P	18	de novo	GeneDx	Campeau et al. (2012), Simpson et al. (2012), Gannon et al. (2015), Zhang et al. (2020)
	K6B_4	c.3769_3772delTCTA, p.Lys1258Glyfs*13	Frameshift	P	18	de novo	Ambry Genetics	Campeau et al. (2012), Simpson et al. (2012), Gannon et al. (2015), Zhang et al. (2020)
	K6B_5	c.3769_3772delTCTA, p.Lys1258Glyfs*13	Frameshift	P	18	U	Invitae	Campeau et al. (2012), Simpson et al. (2012), Gannon et al. (2015), Zhang et al. (2020)
	K6B_6	c.4081_4129dup49, p.Asn1377Argfs*26	Frameshift	P	18	de novo	GeneDx	Zhang et al. (2020)
	K6B_7	c.4102dup, p.Glu1368Glyfs*19	Frameshift	P	18	de novo	Ambry Genetics	
Say-Barber-Biesecker-Young Simpson Syndrome (SBBYSS)	K6B_8	c.3349C>T, p.Gln1117*	Nonsense	P	16	de novo	GeneDx	
	K6B_9	c.3349_3350delCA, p.Gln1117Valfs*19	Frameshift	P	16	de novo	GeneDx	Zhu et al. (2020)
	K6B_10	c.3580C>T, p.Gly1194*	Nonsense	P	17	de novo	GeneDx	
	K6B_11	c.3918_3919insCAACAGG, p.Ile1307Glnfs*4	Frameshift	P	18	de novo	GeneDx	
	K6B_12	c.4205_4206del, p.Ser1402Cysfs*5	Frameshift	P	18	de novo	U	Clayton-Smith et al. (2011), Gannon et al. (2015), Bashir et al. (2017)
	K6B_13	c.4538dup, p.Lys1514Glufs*27	Frameshift	P	18	U	Invitae	
	K6B_14	c.5254C>T, p.Gln1752*	Nonsense	P	18	de novo	GeneDx	
	K6B_15	c.5389C>T, p.Arg1797*	Nonsense	P	18	de novo	Invitae	Clayton-Smith et al. (2011), Szakszon et al. (2013), Gannon et al. (2015), Zhang et al. (2020)

(Continues)

TABLE 1 (Continued)

KAT6B related disorder	Individual	Position of variant on NM_012330.3 reference sequence	Predicted effect of mutation	Pathogenicity	Exon	Inheritance	Laboratory	Variant previously observed in other reported case(s)
Intermediate phenotypes	K6B_16	c.3962_3963delAA, p.Gln1321Argfs*20	Frameshift	LP	18	de novo	UCLA Molecular Diagnostics Laboratory	Gannon et al. (2015), Zhang et al. (2020)
	K6B_17	c.4139_4140delAA, p.Lys1380Argfs*6	Frameshift	P	18	de novo	GeneDx	
	K6B_18	c.4368_4369dup, p.Glu1457Glyfs*5	Frameshift	P	18	de novo	Prevention Genetics	
Not otherwise specified (NOS)	K6B_19	c.4597_4603delGCAACCA, p.Ala1533Trpfs*14	Frameshift	P	18	de novo	Baylor	Clayton-Smith et al. (2011), Niida et al. (2017)
	K6B_20	c.5201_5210del10, p.Met1734Lysfs*87	Frameshift	LP	18	de novo	GeneDx	

Abbreviations: LP, likely pathogenic; P, pathogenic; U, unknown or unspecified.

[a]Reference for coding sequence is NM_012330.3 for *KAT6B*.

for KAT6B were transfected into HEK293T-Cas9 cells using Lipofectamine 3000 (Invitrogen) and the RNAi reverse transfection protocol. Transfected cells were grown for 24–48 h and then serially diluted to obtain single-cell colonies. Single-cell colonies were expanded and DNA was extracted from each clonal line. The region around the guide RNA was amplified from DNA extracted from clonal cell populations and sequenced by Sanger sequencing to confirm the presence of CRISPR-mediated mutations. As HEK cells are pseudotriploid (Bylund et al., 2004), we took into account the potential for mutations across three alleles. Sanger sequencing chromatograms were analyzed using TIDE software to identify CRISPR/Cas9-mediated genetic alterations at *KAT6B* loci (Brinkman et al., 2018). We observed three variants across the two clonal lines and predicted allele count using the TIDE analysis, which was validated by RNAseq of the clonal lines compared to controls. Therefore for Mut1, there is a single mutation affecting one of the three alleles. For Mut2, there are two mutations generated by the same gRNA affecting two of the three alleles (Table S5).

2.5 | RNA-seq library preparation and analysis

RNA was extracted from cells grown to 80%–90% confluence using the PureLink RNA mini kit (Invitrogen #12183018A). Paired-end, 150-bp libraries were prepared at the UCLA Technology Center for Genomics and Bioinformatics Core Facility at UCLA and sequenced on an Illumina HiSeq3000 for an average of 30 million reads per sample. Raw read quality, adaptor content, and duplication rates were assessed with FastQC. Raw reads were then aligned against the Gencode human genome version hg38 (GRCh38) version 31 using STAR 2.7.0e with default parameters (Dobin et al., 2013). Gene counts from raw reads were generated using featureCounts 1.6.5 from the Subread package. For each gene, we counted reads that uniquely mapped to the gene's exons. Differential expression was quantified using DESeq2 v1.24.0 (Love et al., 2014). Genes with an adjusted *p*-value (Benjamini-Hochberg correction) that was <0.05 were considered as significantly differentially expressed (Wald's test). A heatmap was created from normalized counts from the DEseq using R-package heatmap (Kolde, 2015) which shows the top differentially expressed (DE) genes based on log fold-change values >1.5. Color on legend represents normalized counts. The top DE genes are listed in Table S6.

Gene ontology overenrichment tests were completed using clusterProfiler v3.12.0 (Yu et al., 2012) and SetRank v1.1.0 (Simillion et al., 2017). Gene ontology overenrichment tests were completed using clusterProfiler v3.12.0 (Yu

et al., 2012) by submitting differentially expressed genes against all genes from the Gencode hg38. Differentially expressed (DE) genes were tested against a background set of genes created by taking the union of all transcripts that are detected at least once in our entire dataset. A new dataset was created by filtering DE genes for absolute log2FoldChange values ≥1.5. Gene ontologies were classified as significantly enriched when p-adjusted (Benjamini-Hochberg) was <0.05 (hypergeometric test). For overenrichment analysis with the SetRank R package, the unfiltered set of DE genes was tested against the background set of genes and annotated using KEGG Pathways (Rigden & Fernández, 2019) and GO Biological Processes annotations. Cytoscape software (Shannon et al., 2003) was used to visualize the gene set networks returned by SetRank.

2.6 | Chromatin accessibility studies using ATAC-seq

ATAC-seq was performed with 50,000 cells in replicate from wild-type HEK293T-Cas9 cells, and KAT6B-mutated HEK293T-Cas9 cells, as described above. ATAC-seq library generation was performed as described in Corces et al. (2017). Samples were run on the Agilent DNA TapeStation to confirm tagmentation pattern and the genomically barcoded libraries were multiplexed and run on the NextSeq550 with paired-end, 75 bp libraries for a minimum of 30 million reads per sample. The ATACseq FASTQ files were trimmed for adapters using NGmerge Version 0.3 (Gaspar, 2018). The NGmerge output files were assessed for quality using fastqc v0.11.8. Reads were then aligned to the hg38 human reference genome using bowtie2 (Langmead & Salzberg, 2012).

The aligned BAM files were then used to call peaks using Genrich (v0.6) (Gaspar, 2018) and excluding the chrM using −e and the blacklisted regions from GENCODE ENCFF356LFX.bed.gz using −E. The bedgraphish peak files were converted to BEDgraph files and sorted and indexed using samtools. These sorted BED files were then used to create genome-wide read coverage files with the bedGraphToBigWig. The peak file data were further processed to identify differential peaks in case vs control using Diffbind (Stark et al., 2011). The differential peaks were analyzed using DeSeq2 and (FDR <0.05). Chipseeker (Yu et al., 2015) was used to further annotate genomic regions associated with the peaks.

2.7 | Western blotting assay

The cells were harvested using trypsin-EDTA and centrifuged at 500× *g* for 5 min and the cell pellet was washed with PBS. The dry cell pellet was then processed for nuclear and cytoplasmic protein extraction as per the manufacturer's protocol (Thermo Scientific™NE-PER™ Nuclear and Cytoplasmic Extraction Reagents, #78833). For western blotting assay, 10 μg of the nuclear extract protein were loaded on the 4%–15% Criterion™ TGX Stain-Free™ Protein Gel (Bio-Rad #5678083). The protein was transferred to the nitrocellulose (Bio-Rad # 1704271) using a turbo-transfer system, blocked with 1X TBST with 5% nonfat milk for an hour at 4℃, and then incubated with Anti-KAT6B/MORF antibody (Abcam #ab246879, at 0.04 μg/ml) and LaminB1 (Cell Signaling #68591 at 1:200 dilution) overnight. The blots were then washed and detected with IRDye® 800CW secondary antibodies (LI-COR #926-32210 and # 926-32213). All experiments were performed in duplicate.

3 | RESULTS

Our study consisted of 20 individuals with pathogenic variants in the gene *KAT6B* (Table 1). Nineteen cases have not been previously reported in the medical literature, and we have included a case previously described in Clayton-Smith et al. (2011), Gannon et al. (2015), Szakszon et al. (2013), and Zhang et al.'s (2020) recent paper because of their continued care at our institution (K6B_16). Of these 20 cases, 50% (10/20) have new variants not previously described in the literature. Individual age at the time of data collection ranges from 6 months old to 28 years of age and the cohort is 25% male and 75% female. Features shared with at least 50% of individuals in any of the three disease categories are highlighted in Table 2. Herein we present the genotypes and phenotypes of seven individuals classified as having Genitopatellar syndrome, eight individuals classified as having Say-Barber-Biesecker-Young-Simpson syndrome, and five individuals with a combination of features from both classifications.

3.1 | Genotype analysis

Within the 20 cases, we identified 17 different *KAT6B* variants, of which 10 were novel genetic variants. Of the 17 protein-truncating variants reported in this case series, 13 were frameshift variants and four were nonsense variants (Figure 1). Fourteen were found in the acidic domain, two in the serine-rich region, and one in the methionine-rich region of the transcriptional control domain (Pelletier et al., 2002; Figure S2). The mutated variants all fall into a domain that is intrinsically disordered, as defined by both the Espritz (Walsh et al., 2012) and the IUPRED2A (Mészáros et al., 2018) score and these mutations do not

TABLE 2 Major clinical findings found in the 20 individuals with *KAT6B*-related disorders represented in this case series

Feature	GPS (7)	SBBYSS (8)	Intermediate (3)	NOS (2)	Total (20)
Neurological findings					
Developmental delay/intellectual disability	100% (7/7)	100% (8/8)	100% (3/3)	100% (2/2)	100% (20/20)
Profound/severe language impairment	100% (7/7)	100% (7/7)	100% (3/3)	100% (2/2)	100% (19/19)
Delayed mobility/non-ambulatory	100% (7/7)	75% (6/8)	100% (3/3)	50% (1/2)	85% (17/20)
Hypotonia	100% (7/7)	88% (7/8)	100% (3/3)	0% (0/2)	85% (17/20)
Microcephaly	100% (7/7)	63% (5/8)	67% (2/3)	0% (0/2)	70% (14/20)
Agenesis/hypoplasia of corpus callosum	100% (6/6)	14% (1/7)	67% (2/3)	0% (0/2)	50% (9/18)
Cortical visual impairment	80% (4/5)	13% (1/8)	67% (2/3)	—	41% (7/17)
Hearing loss	17% (1/6)	50% (4/8)	33% (1/3)	0% (0/2)	32% (6/19)
Seizures	43% (3/7)	25% (2/8)	0% (0/3)	0% (0/2)	25% (5/20)
Craniofacial features					
Expressionless or "mask-like" faces	—	63% (5/8)	33% (1/3)	0% (0/2)	47% (8/17)
Ptosis	80% (4/5)	75% (6/8)	0% (0/3)	50% (1/2)	61% (11/18)
Strabismus	17% (1/6)	50% (4/8)	67% (2/3)	0% (0/2)	37% (7/19)
Blepharophimosis	—	71% (5/7)	33% (1/3)	50% (1/2)	50% (8/16)
Broad/prominent nasal bridge	71% (5/7)	100% (7/7)	67% (2/3)	0% (0/2)	74% (14/19)
Bulbous nose	100% (6/6)	88% (7/8)	100% (3/3)	0% (0/2)	84% (16/19)
Micrognathia	43% (3/7)	75% (6/8)	67% (2/3)	50% (1/2)	60% (12/20)
Small/pointed/retracted chin	—	75% (6/8)	—	0% (0/2)	73% (11/15)
Bowed and/or thin upper lip and/or small mouth	86% (6/7)	100% (8/8)	33% (1/3)	0% (0/2)	75% (15/20)
High-arched/cleft palate	60% (3/5)	50% (4/8)	67% (2/3)	0% (0/2)	50% (9/18)
Low set/posteriorly rotated/dysplastic ears	100% (6/6)	100% (8/8)	67% (2/3)	50% (1/2)	89% (17/19)
Skeletal features					
Abnormal patella (agenesis/hypoplasia)	100% (6/6)	43% (3/7)	100% (3/3)	0% (0/2)	67% (12/18)
Contractures (knees/hips/club foot)	100% (6/6)	33% (2/6)	100% (3/3)	—	68% (11/16)
Fractures	71% (5/7)	33% (2/6)	0% (0/3)	50% (1/2)	44% (8/18)
Joint hypermobility	—	50% (3/6)	67% (2/3)	50% (1/2)	60% (9/15)
Long thumbs and/or long great toes	83% (5/6)	100% (8/8)	67% (2/3)	0% (0/2)	79% (15/19)
Respiratory issues					
Laryngomalacia/respiratory distress	—	63% (5/8)	100% (3/3)	—	69% (11/16)
Gastrointestinal issues					
Anal stenosis and/or anteriorly placed anus	50% (3/6)	0% (0/8)	0% (0/3)	0% (0/2)	16% (3/19)
Feeding difficulties	100% (7/7)	88% (7/8)	100% (3/3)	100% (2/2)	95% (19/20)
GER/vomiting	50% (3/6)	75% (6/8)	100% (3/3)	50% (1/2)	68% (13/19)
Constipation	43% (3/7)	63% (5/8)	100% (3/3)	0% (0/2)	55% (11/20)
Renal anomalies					
Hydronephrosis	100% (7/7)	17% (1/6)	—	0% (0/2)	47% (8/17)
Genital anomalies					
Genital anomalies	100% (7/7)	38% (3/8)	67% (2/3)	0% (0/2)	60% (12/20)
Male cryptorchidism	100% (2/2)	100% (2/2)	100% (1/1)	—	100% (5/5)
Female hypoplasia of labia minora	80% (4/5)	0% (0/6)	0% (0/2)	0% (0/2)	27% (4/15)
Immunological issues					
Hypothyroidism	20% (1/5)	25% (2/8)	67% (2/3)	50% (1/2)	33% (6/18)

(Continues)

TABLE 2 (Continued)

Feature	GPS (7)	SBBYSS (8)	Intermediate (3)	NOS (2)	Total (20)
Cardiac malformations					
Atrial/ventricular septal defect	86% (6/7)	50% (4/8)	67% (2/3)	—	60% (12/19)
Prenatal findings					
Prenatal anatomy scan findings	100% (6/6)	63% (5/8)	67% (2/3)	—	78% (14/18)
Polyhydramnios	40% (2/5)	50% (4/8)	33% (1/3)	—	41% (7/17)

The main findings previously reported to the literature were used to determine which features to report in the table. Those found in 50% or greater of the cohort or 50% or greater within one specific clinical group are included here, which only includes disease categories with more than four responses on the survey (i.e., yes, no, unknown). A detailed report of all clinical findings for each individual is included in Table S1. (—) indicates a sample size of four individuals or less, therefore not included in this table. If a feature was not appraised (i.e. left blank on the clinical feature survey), the patient was excluded for that feature.

fall into a region of the protein that has a known crystal structure. This might suggest that the mutated domain is critical to complex binding in order to achieve its gene regulatory function.

Consistent with previously reported cases, 100% (7/7) of GPS individuals had variants between amino acids 1150 and 1515 (Zhang et al., 2020) On the other hand, SBBYSS individuals had variants between amino acids 1117 and 1797, intermediate individuals had variants between amino acids 1321 and 1457, and NOS individuals had variants at amino acids 1533 and 1734. Many variants found among our SBBYSS, intermediate, and NOS individuals were clustered in the aspartic acid and glutamic acid-rich region overlapping with previously reported variants for individuals with GPS.

3.2 | Recurrent mutations

Four GPS individuals in our cohort had the same pathogenic variant (K6B_2, K6B_3, K6B_4, K6B_5). Among these four individuals, each had genital anomalies, renal complications, respiratory problems, contractures of knees/hips/elbows/fingers, absent patella, characteristic craniofacial dysmorphology and brain abnormalities, and severe intellectual disability and/or developmental delay. Of note, K6B_2 was most phenotypically similar to K6B_5; both individuals had specific findings such as anal malposition, recurrent UTIs, high anterior hairline, clenched hands, brachydactyly, and obstructive sleep apnea. These clinical findings greatly overlap those reported among the six individuals with the same variant reported in the literature (Clayton-Smith et al., 2011; Gannon et al., 2015; Simpson et al., 2012; Szakszon et al., 2013; Zhang et al., 2020). The enrichment for GPS mutations at this specific genomic and protein position suggests that it is a mutational hotspot.

K6B_16 had a variant classified in 2013 as a likely pathogenic variant associated with SBBYSS but has since been twice reported as GPS and has an intermediate classification within this paper (Gannon et al., 2015; Zhang et al., 2020). Five other individuals (K6B_6, K6B_9, K6B_12, K6B_15, and K6B_20) had variants that were previously reported in the literature and their classifications based upon the (Gannon et al., 2015; Zhang et al., 2020) criteria were concordant with those reports (Bashir et al., 2017; Clayton-Smith et al., 2011; Gannon et al., 2015; Zhang et al., 2020; Zhu et al., 2020). These five individuals had clinical features similar to the individuals reported in the literature with the exception of K6B_20, who lacked every feature appraised in three other individuals with the same variant (Clayton-Smith et al., 2011; Gannon et al., 2015; Niida et al., 2017; Simpson et al., 2012; Szakszon et al., 2013; Zhang et al., 2020).

The molecular mechanisms underlying the positions of the pathogenic variants could support a genetic distinction between GPS and SBBYSS, but the lack of functional data limits our ability to make that conclusion. The immense phenotypic heterogeneity demonstrates the potential to broadly diagnose patients as having a *KAT6B*-spectrum disorder, but additional cohorts of patients need to be phenotyped to assert that there is no clear clinical distinction among individuals with *KAT6B*-related disorders.

3.3 | Clinical features of patients

3.3.1 | Neurodevelopmental and neurological findings

100% (20/20) of the cohort had an intellectual disability or developmental delay. While there is a broad spectrum from mild delay to severe disability seen across our cohort, developmental delay and intellectual disability are expected features (Zhang et al., 2020). Two SBBYSS and one NOS individual had mild intellectual disability. Four GPS, four SBBYSS, three intermediate, and one NOS individual had severe intellectual disability. Three GPS and two SBBYSS individuals had global developmental delay.

Individuals 3 years and older at the time of data collection were either nonverbal (9/12) or delayed in speech or expression (3/12).

All seven GPS individuals, five of the eight SBBYSS individuals, and two of the three intermediate individuals had microcephaly. Nine individuals had agenesis or hypoplasia of the corpus callosum (see Table 2). Three GPS and two SBBYSS individuals experienced seizures (see Table S7). Among those five individuals, 80% (4/5) had appreciable brain abnormalities (Table S7). Major features involving musculature included hypotonia (18/20), appendicular hypertonia (K6B_1, K6B_6), dystonia (K6B_4), spasticity (K6B_5), and dysphagia (K6B_6, K6B_11, K6B_18). Five individuals had behavioral issues, adding to the 12 individuals with behavioral issues recorded in Zhang et al. (2020) (see Table S7). 100% (7/7) of responses on disposition reflected a happy and stable individual.

A total of seven individuals were able to walk at the time of data collection (K6B_9, K6B_10, K6B_12, K6B_14, K6B_16, K6B_19, and K6B_20) and were noted to begin walking as early as 13 months or as late as 8 years old. However, 43% (3/7) of the aforementioned individuals were described as clumsy or had spastic gaits. Two NOS individuals are able to walk (2 years old and 20 years old at the time of data collection), but only one of the three intermediate individuals was able to walk independently (7 yo at time of data collection). The remaining members of our cohort had delays in mobility or were unable to walk at the time of data collection. Of note, 71% (5/7) of GPS individuals were nonambulatory at 2 years of age. 29% (2/7) of GPS individuals were younger than 2 years of age but were still noted to have delayed mobility. The motor impairments and delays in mobility found among GPS individuals in our cohort reflect the severity of motor impairments found among other reports in the literature (Penttinen et al., 2009).

3.3.2 | Visual and hearing impairments

A total of 75% (15/20) of our cohort reported findings related to visual impairment. Of note, four individuals had cortical visual impairments and four individuals had optic nerve hypoplasia. 50% (10/20) of individuals had strabismus, which was further specified as exotropia in three individuals and esotropia in one individual. 100% (3/3) of intermediate individuals and 25% (2/8) of SBBYSS individuals had lacrimal duct anomalies. The additional visual impairments reported in at least one individual are detailed in Table S7. All six individuals with hearing loss also had visual impairments, a finding not well characterized in prior literatures. Of these six, two individuals with SBBYSS (K6B_12, K6B_15) had sensorineural hearing loss, two individuals with SBBYSS (K6B_13, K6B_14) had conductive hearing loss, one GPS individual (K6B_6) had normal auditory sensitivity to slight hearing loss bilaterally, and one intermediate individual (K6B_18) had impaired hearing in one ear. It is unclear if there is a relationship between an individual's *KAT6B*-related disorder and the type of hearing loss that individual has, but identifying hearing loss in 30% (6/20) of our cohort was roughly consistent with the literature on individuals with *KAT6B*-related disorders (Zhang et al., 2020).

3.3.3 | Craniofacial features

The most common facial features found among individuals with *KAT6B*-related disorders assist in the classification of *KAT6B* clinical subtypes while simultaneously demonstrating the overlap among groups in this report. Findings such as immobile, mask-like facies, and blepharophimosis/ptosis are major features suggestive of SBBYSS and were identified in 63% (5/8) and 75% (6/8) of SBBYSS individuals in our cohort, respectively. Immobile, mask-like facies were reported in 25% (3/12) and blepharophimosis/ptosis in 50% (6/12) of all other members of our cohort, illustrating a subtle, yet present, overlap (see Table 2). Photographs depicting the facial features of some individuals included in this case series (see Figure 2).

Features commonly seen across all groups in our cohort include low-set and posteriorly rotated ears (13/20), broad/prominent nasal bridges (15/20), bulbous noses (16/20), and micrognathia with or without retrognathia (16/20). Two GPS and one SBBYSS individuals had bitemporal narrowing, two GPS individuals had brachycephaly, and two SBBYSS individuals had dolichocephaly. One GPS and three SBBYSS individuals had a cleft palate and one SBBYSS individual had a bifid uvula. Two GPS, one SBBYSS, and one intermediate individual had a high-arched palate. 55% (11/20) had thin and sparse eyebrows, a minor anomaly that is likely underreported in cohorts of individuals with *KAT6B*-related disorders. Other features suggestive of a slight facial gestalt include a small mouth with a thin or bowed upper lip (12/20) and a smooth and short (4/20) or long and flat (2/20) philtrum. Additional craniofacial features and ectodermal features are included in Table S7.

A number of dental anomalies were identified among seven individuals. Three of the four GPS individuals with the same p.Lys1258Glyfs*13 variant had delayed tooth eruption; K6B_2 had hypoplastic teeth, K6B_4 had hypoplastic teeth and mildly discolored, small teeth, and K6_5 had an underbite. Additional dental findings include dental overcrowding (K6B_12), widely spaced, peg-shaped, hypoplastic teeth (K6B_14), a pointed mandible

at the symphysis (K6B_15), and mildly hypoplastic teeth (K6B_16).

3.3.4 | Skeletal features

All individuals reported here had one or more skeletal abnormality, with high variability in this category. The abnormal patella, one of the characteristic skeletal findings among *KAT6B*-related disorders, was identified in 60% (12/20) of our cohort. 86% (6/7) of GPS individuals had agenesis of their patellae. Hypoplastic patellae were reported in 50% (3/6) of SBBYSS individuals and 100% (3/3) of intermediate individuals. Contractures of the knees and/or hips and/or club feet, a characteristic finding among GPS individuals, were identified in six GPS individuals, three SBBYSS individuals, and three intermediate individuals. Skeletal features more characteristic of SBBYSS include long thumbs and/or long great toes, which was found in 100% (8/8) of SBBYS individuals in our cohort. Thorax anomalies across one intermediate, two SBBYSS, and three GPS individuals include mild pectus excavatum, pectus carinatum, wide-set nipples, inverted nipples, low-set nipples, short sternum, and long neck. Less commonly identified skeletal features found in one or more individuals are included in Table S7.

Joint hypermobility, dislocations, and fractures were all skeletal findings reported at a higher frequency in our cohort compared with previously described cases (Zhang et al., 2020). 45% (9/20) had joint hypermobility (see Table 2), though the location of the joint hypermobility was only specified in three individuals (see Table S7). Two GPS individuals had bilateral hip dislocations, and one GPS and one intermediate individual had bilateral patellar subluxations. Five GPS individuals had fractures, with 60% (3/5) reporting fractures in either the femur or tibia. Three of these five GPS individuals had more than one fracture, though their ages at the time of these fractures are unknown. SBBYSS individual K6B_10 had a right tibia and fibula fracture after a fall at 3 years old, SBBYSS individual K6B_15 had a right femur and tibia fracture, and NOS individual K6B_19 had a tibia and fibula fracture at 7 years old and a femur fracture at 8 years old. The photographs provided in Figure 2c depict the major skeletal features surveyed by clinicians.

3.3.5 | Gastrointestinal problems

Feeding difficulties were reported in all but one member of the cohort (19/20). These included gastrostomy tube dependence (11/20), gastro-jejunal tube feeding (2/20), Nissen fundoplication (1/20), nasogastric intubation neonatally (1/20), failure to thrive (2/20), and feeding issues present only at birth (1/20). Gastroesophageal reflux and/or disease was found in 13 individuals but was resolved in 23% (3/13) of those individuals. Constipation was also a commonly reported finding identified in half of our cohort (10/20). Four GPS individuals had small bowel malrotation, including two with malrotation status post-Ladd's procedure (K6B_1, K6B_6). Anal anomalies, a more severe finding typically found in GPS individuals (Zhang et al., 2020), were reported in three GPS individuals and include anteriorly placed anus and anal stenosis or proximally placed anus. Other gastrointestinal problems are listed on Table S7.

3.3.6 | Cardiac malformations

Seventy-five percentage (15/20) of individuals included in this cohort were reported to have a congenital heart defect. The most common congenital heart defects found within our cohort include atrial septal defects (9/20), ventricular septal defects (4/20), patent ductus arteriosus (6/20), and small patent foramen ovale (1/20), which are all consistent with the data from previous reports on patients with *KAT6B*-related disorders provided by (Zhang et al., 2020). Additional cardiac malformations found in at least one individual in our cohort are detailed in Table S7.

3.3.7 | Renal, immunological, and urogenital anomalies

Kidney abnormalities that persist beyond the prenatal period were predominantly identified in GPS individuals within our cohort. All seven GPS individuals had hydronephrosis. Although three other individuals were reported to have hydronephrosis, theirs was resolved postnatally. Five GPS individuals were reported to have kidney abnormalities including bilateral ureteropelvic junction obstruction (1/5) and a malrotated right kidney (1/5). Two individuals had multicystic kidneys (K6B_6 and K6B_18) and one individual had dysplastic kidneys (K6B_7).

GPS individuals K6B_2, K6B_4, and K6B_5 had recurrent urinary tract infections, requiring surgical interventions such as ureter surgery with input and output catheterization in K6B_4 and pyeloplasty and stent insertion in K6B_5. Recurrent ear infections were identified in SBBYSS individuals K6B_9 and K6B_14 and intermediate individual K6B_16. Though one GPS and one NOS individual had hypothyroidism that was resolved shortly after birth (2/6), hypothyroidism was more commonly identified in SBBYSS (2/6) and intermediate (2/6) individuals.

All five males within the cohort (two GPS, two SBBYSS, and one intermediate) had genital anomalies. Cryptorchidism

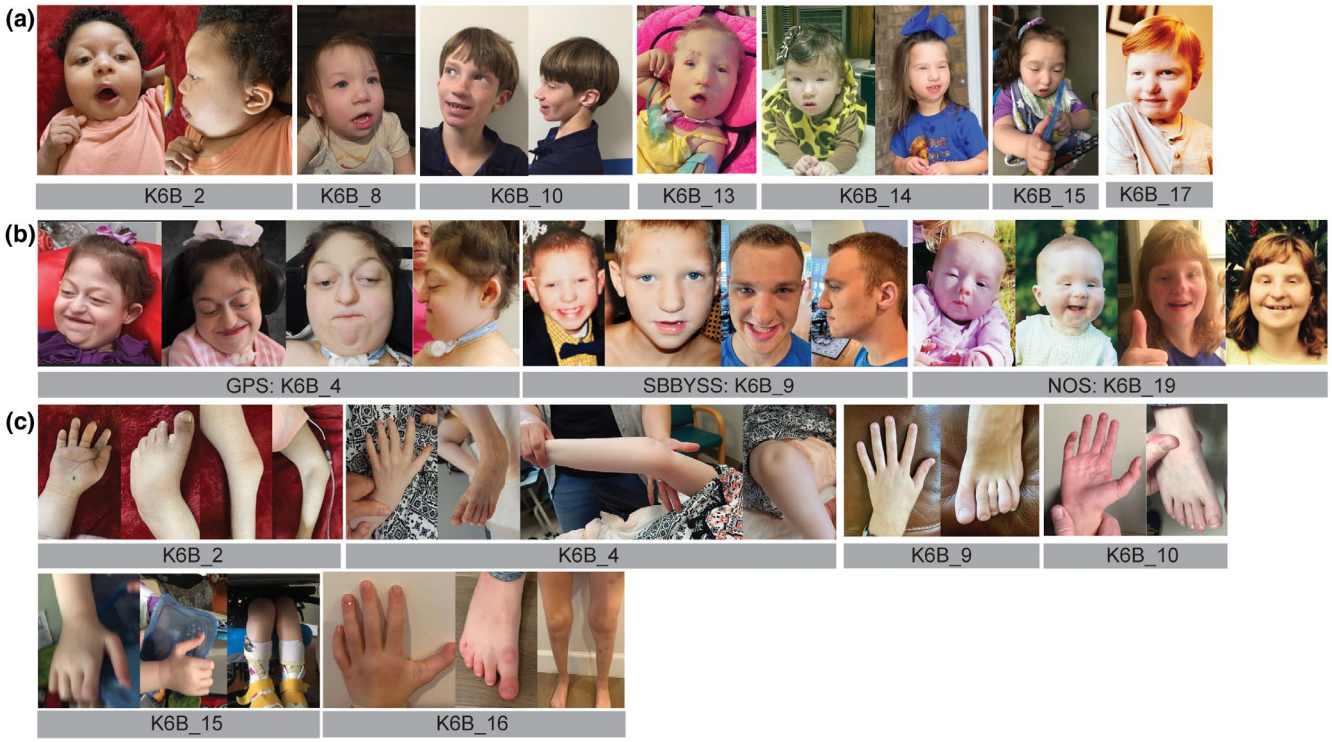

FIGURE 2 *KAT6B*-related facial features and skeletal anomalies in our cohort. (a) Facial features within three *KAT6B*-related clinical groups (Genitopatellar Syndrome—GPS, Say-Barber-Biesecker-Young-Simpson Syndrome—SBBYSS, intermediate, and not otherwise specified—NOS). Note the microcephaly, bitemporal narrowing, bowed and/or thin lips, ptosis, bulbous nasal tip, and dysplastic ears in GPS individual K6B_2 and SBBYSS individual K6B_15. Note the "mask-like" facies, blepharophimosis, ptosis, and bulbous nose in SBBYSS individuals K6B_8, K6B_13, and K6B_14. Note the variable and milder dysmorphic features including blepharophimosis and bulbous nasal tip in SBBYSS individual K6B_10 and intermediate individual K6B_17. (b) Comparison of facial features evolving with age in each clinical group in our cohort. K6B_4 (GPS) persisted in having retromicrognathia with age. Note milder ocular features in K6B_9 (SBBYSS) whose bulbous nasal tip becomes the predominant dysmorphic feature with age. Note how blepharophimosis and ptosis persist with age in K6B_19 (NOS) and how the bulbous and bifid nasal tip became more evident with age. Note that K6B_9 (SBBYSS) and K6B_19 (NOS) presented with retromicrognathia at an earlier age, developing more prognathism with mild underbite with age. (c) Skeletal survey of major features. Top Row (from left to right): K6B_2 with mild brachydactyly with partial proximal syndactyly of all digits, long great toe, and absent patella; K6B_4 with finger contractures, long feet and great toes, elbow contracture, and absent patella; K6B_15 with long thumbs and absent patella. Bottom Row (from left to right): Long digits and thumbs, long great toes, and hypoplastic patellae (K6B_9, K6B_10, K6B_16)

was seen in all five males, requiring one to undergo a right orchiopexy at a young age. Additionally, scrotal hypoplasia was reported in one and hypospadias was reported in two males. Four GPS females had hypoplasia of the labia minora, a finding not seen across any other individuals with *KAT6B*-related disorders in our cohort. Other genital anomalies identified among the cohort are detailed in Table S7.

3.3.8 | Respiratory problems

In this cohort, 55% (11/20) of individuals were reported to have laryngomalacia and/or respiratory distress. Of these 11 individuals, five had obstructive sleep apnea or severe sleep-disordered breathing (two GPS, two SBBYSS, and one intermediate). Four young individuals ranging from 6 months old to almost 3 years old at the time of data collection had chronic lung disease; 75% (3/4) were born prematurely. Individual K6B_4 was born at 32 weeks gestation and experienced chronic respiratory insufficiency, remaining tracheostomy dependent and vent dependent at night with a BiPAP machine at 13 years old. To aid in the management of respiratory problems, three individuals were placed on oxygen (K6B_5, K6B_11, and K6B_18) and four individuals had a tracheostomy (K6B_3, K6B_4, K6B_13, and K6B_17). Additional problems reported in one or more individuals are included on Table S7.

3.3.9 | Prenatal findings

Prenatal anomalies are frequently identified before the individual is born (Zhang et al., 2020). Prenatal anatomy scans in our cohort included increased nuchal translucency

(K6B_5 and K6B_14) and polyhydramnios (two GPS, four SBBYSS, and one intermediate). The other common prenatal finding was hydronephrosis, which was identified in 35% (7/20) of our cohort. Only two cases of hydronephrosis were resolved prenatally (K6B_12 and K6B_16), while hydronephrosis persisted postnatally in the other five individuals. Additional congenital anomalies identified prenatally included club foot (5/20), congenital heart defects (4/20), and agenesis of the corpus callosum (3/20). Other anomalies noted prenatally are detailed in Table S7.

3.4 | Additional clinical features

A summary of all clinical features described is shown in Table S1 and includes unique features seen in a few patients. Some of these clinical findings may not alter the overall treatment and management of individuals with *KAT6B*-related disorders, but detailing these findings may prove to be beneficial when identifying additional findings in larger cohorts. For example, low bone density in K6B_4, osteopenia in K6B_6, subluxation and ossification delay of proximal femoral epiphyses in K6B_15, and high pain tolerance in K6B_16 might help explain the higher incidence of fractures seen in our cohort and should be carefully examined for in other patients with *KAT6B*-related disorders. Additionally, the interesting findings of photophobia in K6B_4 and sneezing in the sun and significant hypersensitivity to noise in K6B_16 might be underappreciated in our cohort and should be investigated to provide individuals more comfort in daily living. K6B_3 was identified to have adrenal insufficiency, though no additional details were provided. Other findings found in only one individual within our cohort are included in Table S7.

3.5 | Role of genetic counseling offered to patients with *KAT6B*-related disorders

To assess the role of genetic counselors in the care and management of individuals diagnosed with *KAT6B*-related disorders, we appended a list of genetic counseling-related questions to the comprehensive clinical phenotypic survey. We anticipated that the immense heterogeneity among *KAT6B*-related disorder phenotypes would pose unique challenges in the way providers manage the vast uncertainties that arise.

We received 18/20 responses to our genetic counselor involvement survey (Table S2). Ninety-four percentage (17/18) of individuals and their families met with a genetic counselor for one to four sessions (Figure 3a). Individuals received a diagnosis of a *KAT6B*-related disorder between 6 weeks old and 22 years old with the majority, 56% (10/18), having their first visit before 3 years of age (Figure 3b). Overall, individuals and/or their families benefited from the genetic counselor's role in coordinating testing, obtaining consent for testing, delivering the results from testing, counseling leading up to and following diagnosis, and coordinating follow-up care (Figure 3c). The majority of individuals and/or their families were receptive to the information given at diagnosis and were grateful to find an answer they have been looking for, a consistent outcome despite the range of ages and phenotypes among the cohort (Figure 3d).

Many families sought additional information about the prognosis, recurrence risk, and concerns for other medical complications, which are all interconnected and further complicated by the limited information about prognosis and resources available (Figure 3e,f). The biggest challenge genetic counselors faced when relaying information about the condition to the family resulted from the varying phenotypes and complexity of *KAT6B*-related disorders (Figure 3f). This overarching challenge encompasses the desire to have a clear genotype–phenotype correlation, frustration surrounding individuals with milder phenotypes than what is found in the literature, and questions about the different phenotypes. For example, the genetic counselor in K6B_14's case was hesitant to give the family information on support/Facebook groups because of the frustration expressed about the individual's lack of major features found within the literature. The eldest individuals were glad to have a specific genetic diagnosis after so many years, but the genetic counselors involved in their care noted that there were no condition-specific family organizations and limited family friendly information available. The wide array of educational and external resources offered to the families of individuals depict the variegated needs of *KAT6B*-related disorder patients with heterogeneous phenotypes (Table S2).

3.6 | Truncating *KAT6B* mutations alter gene expression for transcripts controlling RNA biogenesis and metabolism

To explore the role of *KAT6B* truncating mutations on RNA expression, we transfected HEK293T-Cas9 AAVS1 (GeneCopoeia) cell lines with CRISPR guide RNAs targeted to *KAT6B* gene (Table S4, Integrated DNA Technology). Single-cell clones were then selected and grown-up to identify multiple clonal lines harboring *KAT6B* mutations. HEK cells are pseudotriploid (Bylund et al., 2004) and we introduced indel mutations within exon 3 of the *KAT6B* gene (Figure 4a, Table S5). These mutations are all predicted to result in a frameshift

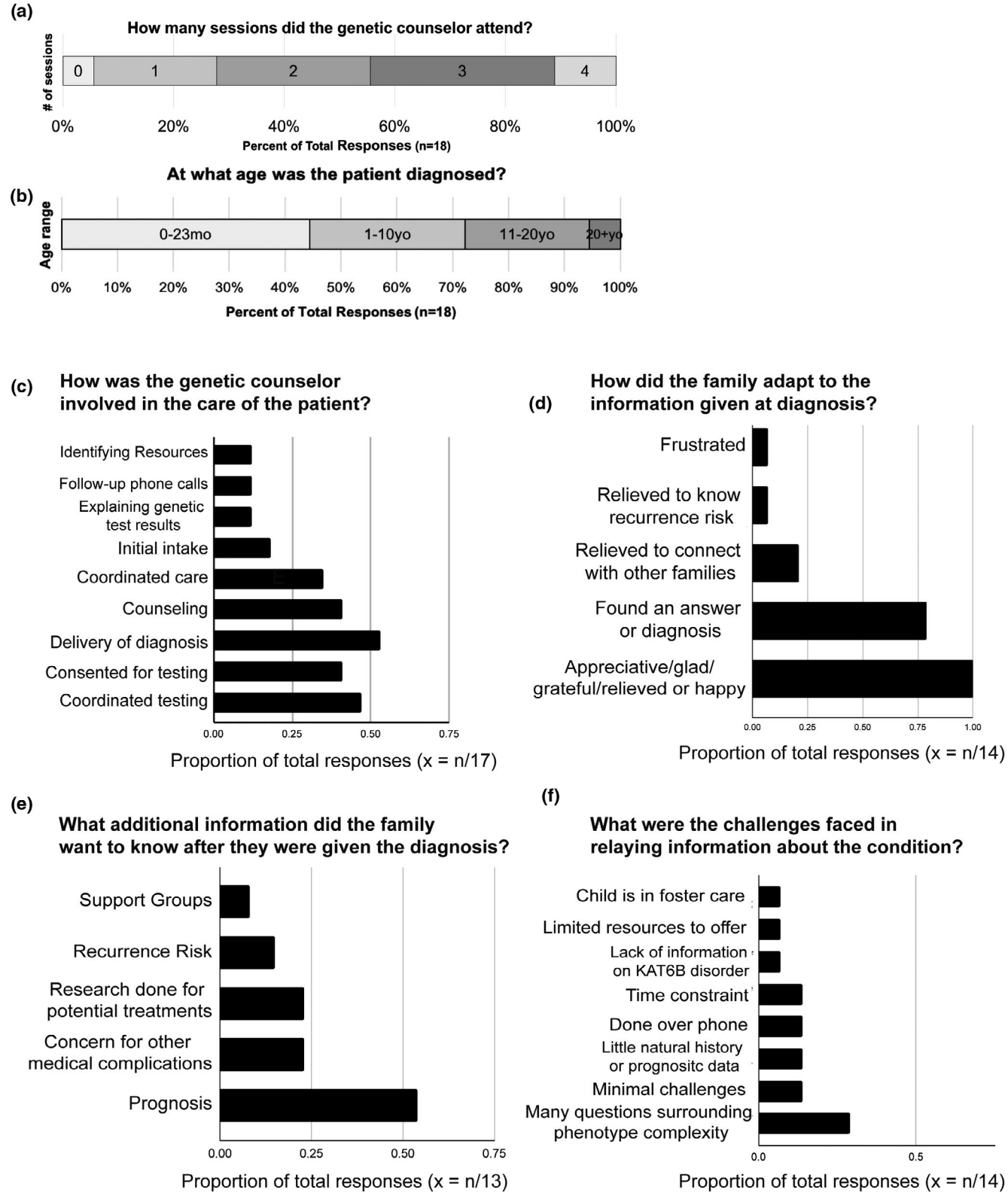

FIGURE 3 Genetic Counseling support related to the care and management of patients. (a) Of the 18 respondents, a genetic counselor was present for 0–4 sessions involving the team involved in the care of the patient. (b) Individuals received a diagnosis of a KAT6B-related disorder as early as 6 weeks old to as late as 23 years old. (c) Typical roles and responsibilities that genetic counselors hold demonstrate consistency despite the heterogeneous nature of patients with mutations in *KAT6B*. (d) Overall, patients and their families were receptive to the information given at diagnosis and relieved to have a diagnosis. (e) Many families sought additional information about the likely or expected development of disease with extra concern for future medical complications. (f) Due to the phenotypic heterogeneity found among patients with pathogenic variants in *KAT6B*, a wide variety of challenges arose when relaying information about the condition to the family

protein and truncation. DNA extracted from each clonal line was amplified, TOPO-cloned, and 10 colonies underwent Sanger sequencing to identify the *KAT6B* mutations present. These mutations introduced frameshift mutations into the coding DNA and were predicted to result in protein truncation.

We sought to first determine whether the primary effect of the *KAT6B* mutations altered chromatin accessibility, gene expression, or both. Therefore, we performed ATAC-seq and RNA-sequencing on each of the clonal lines and compared them to that of the control HEK293T-Cas9 cells. For both analyses, we tested 2 biological replicates of each cell line.

We first explored the effect of the introduced *KAT6B* mutations on chromatin accessibility using ATAC-seq (Figure S4a). Surprisingly, our analysis identified only 16 differential peaks between *KAT6B* cases and controls at an FDR of 0.05. (Figures S4b,c, Table S6). Our data suggest that there are very limited changes to the chromatin accessibility between the mutated and control cell lines.

Using the RNA sequencing data, we confirmed our Sanger sequencing results of the *KAT6B* mutations and demonstrated the presence of the truncating mutations into exon 3 and are predicted to fall 5' to the histone acetyltransferase domain. We next sought to determine whether the mutations resulted in decreased gene or protein expression. Our data showed that the cell lines showed a 2.43-fold decrease in *KAT6B* expression in both mutant cell lines evaluated (Figure S3a). No significant differences in KAT6B transcript levels were observed between Mut1 and Mut2, which had one or two *KAT6B* mutations, respectively. However, western blot analysis did not show a measurable change in KAT6B protein expression in our mutant lines (Figure S3b).

We next explored whether there were significant changes to gene expression. Differential gene expression analysis identified 954 genes that were differentially expressed after correction for multiple testing (Table S8). Of these, 434 of the significant genes showed a fold change of 1.5 or greater and we observe clustering of the signal between replicates and concordant differences between samples that were controlled versus mutant lines (Figure 4b and Figure S5). Of the significantly differentially expressed genes with an absolute fold change of 1.5 or greater, the two largest groups consisted of protein-coding mRNAs which represented 92.4% ($n = 401/434$) of transcripts and long-noncoding RNAs representing 4.14% ($n = 18/434$).

Our experimental studies have shown a decrease in mRNA levels but no concomitant decrease in protein expression. Therefore, we cannot conclude that haploinsufficiency is the mechanism of action. However, we cannot rule out the possibility that our western blot analysis may not be sensitive enough to mild-to-moderate decreases of protein expression. We observe very minor differences in chromatin accessibility in our studies suggesting that the introduced mutations do not significantly affect chromatin accessibility. This is surprising given the known role in KAT6B histone acetylation, but suggests that the mechanisms of effect of the *KAT6B* mutations are not through alteration of chromatin accessibility.

To identify pathways that are significantly enriched, we used genes with a fold change of 1.5 or greater and performed a gene ontology enrichment analysis to determine if these genes identified common pathways. We observed significant enrichment in gene sets associated with osteoblast differentiation, axon development, and urogenital development (Figure 4c). These, and other processes, are consistent with the common clinical phenotypes of *KAT6B*-related syndromes such as higher incidence of fractures, skeletal anomalies, intellectual disability, and kidney (metanephros) anomalies. Analysis for the enrichment of biological processes has identified common metabolism pathways highlighting Coenzyme A biosynthetic processes and the regulation of developmental processes (Figure S6). The utility of in vitro cell models to unravel gene regulatory pathways underlying these rare diseases can be used as a step toward linking our understanding of gene regulatory mechanisms and clinical phenotypes for these exceedingly rare disorders.

4 | DISCUSSION

As the number of rare genetic syndromes continues to expand, and the simple classical model associated with rare pathogenic variants continues to expand, we find that the phenotypic spectrum within a gene (Arboleda et al., 2012; Borges et al., 2015), the oligogenic genetic variation that results in the same clinical phenotypes (Badano et al., 2006; Shaw et al., 2017), or that the presence of multiple independent and distinct syndromes in the same individual lead to an "atypical" presentation (Posey et al., 2017). Both the expansion of the spectrum of pathogenic variants and the syndromic changes with age allows areas that are experiencing explosive growth in our knowledge to promote greater understanding within clinical genetics. The cases presented here span a relatively wide age range and allowed us to perform a comprehensive phenotype assessment to elucidate the clinical phenotypes in childhood, adolescence, and early adulthood. These aspects are essential for young and newly diagnosed individuals to understand and potentially predict what the phenotypic spectrum is throughout the phases of life, an aspect of medical genetics that is not as well characterized.

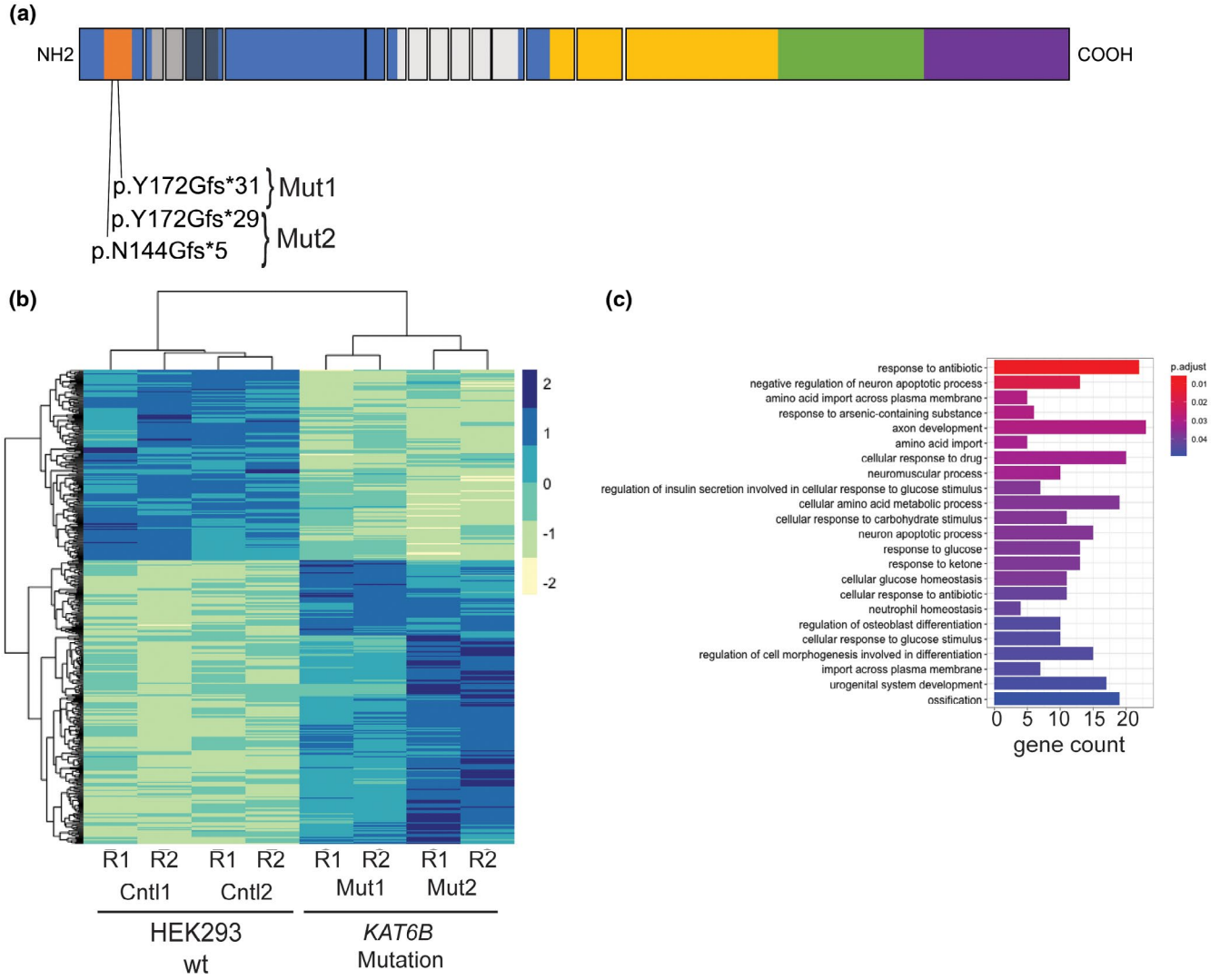

FIGURE 4 *KAT6B* mutations in HEK293T cells result in dysregulation of relevant gene regulatory pathways. (a) For each of the *KAT6B*-mutant cell lines generated by Cas9-CRISPR, we sequenced genomic DNA and cDNA to identify allelic mutations in each line. The mutations are predicted to result in frameshift mutations resulting in protein truncation. Mut1 cell line has a single mutation, whereas Mut2 has two independent mutations on three alleles. (b) Heat map comparing counts for all differentially expressed genes with fold-change >1.5 and FDR <0.5 (n = 434 genes). We compared our HEK293 control cells (C1 and C2) and the cells with *KAT6B* mutation (Mut1 and Mut2). (c) Differentially expressed genes were found to be significantly enriched in core features related to *KAT6B* clinical syndrome including skeletal ossification, urogenital development, axonal development. The *X*-axis demonstrates the number of differentially expressed genes that are within each category on the *Y*-axis. The color of the bar represents the adjusted p-value for the enrichment

The broad expanse of phenotypic findings presented in this report demonstrates the importance of the multi-system approach to the physical exam. The prognosis for genetic conditions that are highly variable in presentation can be difficult to determine without a broader understanding of the evolution of symptomatology over time in a larger and well-phenotyped cohort. The identification of both novel and well-characterized clinical features within our cohort demonstrates that a holistic evaluation is critical to the establishment of long-term care. Uncovering findings, such as concern for keratoconus, sensitivity to light or noise, recurrent infections, and a higher incidence of fractures point to additional complications that might otherwise be attributed to common childhood accidents or anecdotes. Aside from these findings, joint hypermobility, hypothyroidism, polyhydramnios, and seizures were reported in greater numbers than previously reported in GPS, SBBYSS, intermediate, and NOS presentations.

The clinical findings identified within this study require follow-up screenings for management and, potentially, treatment. Regular visual assessments are recommended, especially referrals to ophthalmology when strabismus,

ptosis, and cortical visual impairments are identified. Due to the higher incidence of fractures among our cohort, it may be necessary to perform bone densitometry testing to monitor bone health in childhood. This is especially necessary for children who have already fractured a bone. 100% (20/20) of individuals had feeding difficulties and other gastrointestinal issues, pointing to the critical importance of monitoring feeding and bowel movements throughout infancy. In our cohort, 75% (15/20) of individuals had congenital heart defects. For this reason, we recommend all individuals with a diagnosis of a *KAT6B*-related disorder have an electrocardiogram and an echocardiogram. The incidence of hypothyroidism points to the implementation of thyroid-stimulating hormone blood tests shortly after diagnosis. And, finally, a sleep study would be helpful to investigate abnormal breathing patterns and whether additional breathing support while sleeping is necessary.

While there is support for eliminating the strict GPS and SBBYSS classifications in favor of *KAT6B*-spectrum disorders, there are still patterns of features that serve to differentiate the two conditions (renal, anal, genital, skeletal (absent patella) features [GPS]; characteristic facies [SBBYSS]). Highlighting these findings help provide anticipatory guidance for families seeking more information on what to expect. Thus, recognizing the clinical heterogeneity found among cohorts receiving *KAT6B*-related diagnoses is critical for supporting individuals throughout their diagnostic odyssey. At the start of this study, we aimed to have all families revisit their physician for updated phenotyping and examination. However, some patients could not be assessed in person due to pandemic restrictions limiting the identification of additional features that were more recently described in Zhang et al. (2020) such as cystic hygroma and increased nuchal translucency prenatally as well as optic nerve hypoplasia.

The field of genetic counseling has, with increased genomic testing, continued to expand. Our goal was to quantify our awareness of difficulties faced when addressing common patient inquiries to improve genetic counselor support. The rapid pace of genetics research, novel rare disease gene discovery, and the increasing interconnectedness of the patient families through social media have largely improved our understanding of these exceedingly rare disorders. The diagnostic journey is often led by genetic counseling professionals and understanding how the clinical needs for these rare disease patient families evolve over time is critical as we encounter more and more disorders that are defined by their phenotypic variability and linked by a genetic diagnosis.

As these rare disease cohorts continue to grow and new therapies start being tested, the role of the genetic counselor continues to evolve. Continually evaluating where families need support, particularly beyond the patient's diagnostic odyssey, remains a critical component to the improvement of this nascent field's role in guiding the patient through difficult conversations about prognosis and ultimately, we hope, therapies. Developing qualitative and quantitative metrics to track patient needs remains challenging as there are thousands of clinical disorders and our knowledge about each disorder and its progression in patients is dependent on the clinical research literature. Reporting of cases in older patients with longer clinical history remains a critical need as the field of medical genetics continues to expand its role from diagnosis to include prognosis and treatment.

A limitation of our study on genetic counselor involvement is that we did not directly survey the families and relied on the assessment of the clinicians involved to quantify the genetic counselor role. In future surveys, it would be more informative to assess a large cohort of families directly who had recently interfaced with their clinical team and genetic counselor. These studies can be more easily facilitated by the presence of social media groups that can rapidly disseminate these surveys. Larger sample size would enable a more quantitative assessment of the evolving needs of rare disease patients and their families, particularly with the increasing availability of genetic-based treatments (Mendell et al., 2016; Miller & Humer, 2019; Wainwright et al., 2015).

Since the first identification of *de novo* truncating variants in *KAT6B* as the cause for GPS and SBBYSS, there have been many additional reports of cases and clinical phenotypes expanding the clinical spectrum around *KAT6B*-related disorders. Given the short time frame here, we recognize that these patients have received a diagnosis while our understanding of the gene and its clinical phenotypes have simultaneously expanded. Thus, assessing the efficacy of the diagnostic process and the role of genetic counselors is particularly challenging in the constant evolution of the *KAT6B*-spectrum. For genetic counselors, deciding what resources are appropriate for a patient reflects both the challenges a family faces in providing care and the severity of the clinical features found within the *KAT6B*-related disorder spectrum.

As we associate pathogenic variants with clinical phenotypes, there is a need to link the analysis of the effect of the variant on molecular and cellular phenotypes and how that contributes to the ultimate clinical phenotypes we observe. This is particularly important in genes that can have different effects depending on the location and type of variant observed. This is seen in several genes including *CDKN1C* (Arboleda et al., 2012; Borges et al., 2015) associated with IMAGe Syndrome and Beckwith Wiedemann Syndrome, and *TGFBR1* (Goudie et al., 2011) associated with both Ferguson-Smith disease (FSD) and Marfan syndrome-related disorders. The phenotypic

spectrum associated with pathogenic variants in *KAT6B* reflects the complex interactions of genetic variants in a single gene with cellular complexes.

There are several key limitations to our cell-based studies. First, the CRISPR-Cas9 editing introduces random indels which are predicted to result in frameshift mutations and protein truncation before the histone acetyltransferase domain. Therefore, the mutations are located 5' to the majority of mutations that are identified in *KAT6B*-spectrum disorder. Another limitation is the use of the HEK293 cell line, which is a triploid, and transformed cell line that is derived from the human embryonic kidney. The embryonic kidney is affected in the *KAT6B*-spectrum disorders and has moderate mRNA and protein expression (Figures S3a,b) suggesting that decreased expression should have an effect on molecular phenotypes. We chose to use HEK293 cell line in order to isolate the *KAT6B* mutation on isogenic lines rather than obtaining cell lines from affected individuals, where the genetic background could have an undue influence on transcriptomic and chromatin accessibility profiling. Future studies with prime-edited lines representing specific patient mutations, in both stem cell lines and animal models, would further expand our knowledge of how truncating *KAT6B*-spectrum mutations can give rise to distinct clinical features.

We make the intriguing observation that there are few significant changes to chromatin accessibility in our HEK293 cells but significant changes to gene expression in our model system. This suggests that the effect of introduced *KAT6B* mutations acts to change the transcriptional activation domains of the KAT6B and/or to effect posttranslational modifications of transcription factors. However, the origin of the observed transcriptional changes is confounded by the triploid nature of the cell model system. Gene ontology enrichment analyses can identify presence of genes associated with known pathways and can provide some data on processes that are altered by the dysregulated gene set. Early experiments like the ones included here may help in identification of key relevant pathways that may be activated or dysregulated in the presence of a *KAT6B* mutation. These mechanisms are worthy of additional exploration using expanded CRISPR-based screening.

As we continue to identify novel pathogenic variants across genes and expand the phenotypic spectrums associated with these variants, we must consider that we are shifting from ending the diagnostic odyssey to preparing individuals for their child's evolving needs and toward an understanding of the trajectory of diseases. Understanding the natural progression of a genetic disorder is a key aspect when developing therapies—as one needs to have a metric by which to measure phenotypic improvement in the disease state. Thus, continual identification of the clinical spectrum but also the evolution of medical needs over time remains critical to developing a complete understanding of the disease progression to enable safe and effective therapies.

ACKNOWLEDGEMENTS

We thank all the patients and families who participated in this study. We acknowledge the UCLA Technology Center for Genomics & Bioinformatics (TCGB) Core for their sequencing capabilities. This work was supported by NIH Grant DP5OD024579 to VA.

CONFLICT OF INTEREST

The authors declare no conflict of interest.

AUTHOR CONTRIBUTIONS

MY, JK, DS, VA conceptualized the study and designed the survey for clinicians. MY analyzed the data and MY and VA wrote the manuscript with significant input from JK and DS. AW, MS, and MFP did formal analysis. KE and MS performed experimental investigations. All co-authors investigated the patients in their care and collected deidentified data for analysis. All co-authors approved the manuscript.

ETHICS DECLARATION

This project was approved by the UCLA IRB#20-000798. All individual-level data were deidentified prior to analysis. Any photos included here were obtained and included with patient consent.

DATA AVAILABILITY STATEMENT

The data that support the findings of this study are being submitted into a publicly available repository in SRA hosted by NIH. The Reference Numbers are pending.

ORCID

Meghan C. Towne https://orcid.org/0000-0001-9460-2368
John M. Graham Jr. https://orcid.org/0000-0003-4297-1078
Valerie A. Arboleda https://orcid.org/0000-0002-9687-9122

REFERENCES

Arboleda, V. A., Lee, H., Parnaik, R., Fleming, A., Banerjee, A., Ferraz-de-Souza, B., Délot, E. C., Rodriguez-Fernandez, I. A., Braslavsky, D., Bergadá, I., Dell'Angelica, E. C., Nelson, S. F., Martinez-Agosto, J. A., Achermann, J. C., & Vilain, E. (2012). Mutations in the PCNA-binding domain of CDKN1C cause IMAGe syndrome. *Nature Genetics*, *44*(7), 788–792. https://doi.org/10.1038/ng.2275

Avvakumov, N., & Cote, J. (2007). The MYST family of histone acetyltransferases and their intimate links to cancer. *Oncogene*, *26*(37), 5395–5407. https://doi.org/10.1038/sj.onc.1210608

Badano, J. L., Leitch, C. C., Ansley, S. J., May-Simera, H., Lawson, S., Lewis, R. A., Beales, P. L., Dietz, H. C., Fisher, S., & Katsanis, N.

(2006). Dissection of epistasis in oligogenic Bardet-Biedl syndrome. *Nature*, *439*(7074), 326–330. https://doi.org/10.1038/nature04370

Bashir, R. A., Dixit, A., Goedhart, C., Parboosingh, J. S., Innes, A. M., Care for Rare Canada Consortium, Ferreira, P., Hasan, S. U., & Au, P. Y. (2017). Lin-Gettig syndrome: Craniosynostosis expands the spectrum of the KAT6B related disorders. *American Journal of Medical Genetics Part A*, *173*(10), 2596–2604.

Biesecker, L. G. (1991). The Ohdo blepharophimosis syndrome: A third case. *Journal of Medical Genetics*, *28*(2), 131–134. https://doi.org/10.1136/jmg.28.2.131

Borges, K. S., Arboleda, V. A., & Vilain, E. (2015). Mutations in the PCNA-binding site of CDKN1C inhibit cell proliferation by impairing the entry into S phase. *Cell Division*, *10*, 2. https://doi.org/10.1186/s13008-015-0008-8

Brinkman, E. K., Kousholt, A. N., Harmsen, T., Leemans, C., Chen, T., Jonkers, J., & van Steensel, B. (2018). Easy quantification of template-directed CRISPR/Cas9 editing. *Nucleic Acids Research*, *46*(10), e58. https://doi.org/10.1093/nar/gky164

Bylund, L., Kytölä, S., Lui, W.-O., Larsson, C., & Weber, G. (2004). Analysis of the cytogenetic stability of the human embryonal kidney cell line 293 by cytogenetic and STR profiling approaches. *Cytogenetic and Genome Research*, *106*(1), 28–32. https://doi.org/10.1159/000078556

Campeau, P. M., Kim, J. C., Lu, J. T., Schwartzentruber, J. A., Abdul-Rahman, O. A., Schlaubitz, S., Murdock, D. M., Jiang, M.-M., Lammer, E. J., Enns, G. M., Rhead, W. J., Rowland, J., Robertson, S. P., Cormier-Daire, V., Bainbridge, M. N., Yang, X.-J., Gingras, M.-C., Gibbs, R. A., Rosenblatt, D. S., … Lee, B. H. (2012). Mutations in KAT6B, encoding a histone acetyltransferase, cause genitopatellar syndrome. *American Journal of Human Genetics*, *90*(2), 282–289. https://doi.org/10.1016/j.ajhg.2011.11.023

Cavalcanti, D. P. (1989). Unknown syndrome: Abnormal facies, hypothyroidism, postaxial polydactyly, and severe retardation: A third patient. *Journal of Medical Genetics*, *26*(12), 785–786. https://doi.org/10.1136/jmg.26.12.785

Champagne, N., Pelletier, N., & Yang, X. J. (2001). The monocytic leukemia zinc finger protein MOZ is a histone acetyltransferase. *Oncogene*, *20*(3), 404–409. https://doi.org/10.1038/sj.onc.1204114

Clayton-Smith, J., O'Sullivan, J., Daly, S., Bhaskar, S., Day, R., Anderson, B., Voss, A. K., Thomas, T., Biesecker, L. G., Smith, P., Fryer, A., Chandler, K. E., Kerr, B., Tassabehji, M., Lynch, S.-A., Krajewska-Walasek, M., McKee, S., Smith, J., Sweeney, E., … Black, G. (2011). Whole-exome-sequencing identifies mutations in histone acetyltransferase gene KAT6B in individuals with the Say-Barber-Biesecker variant of Ohdo syndrome. *American Journal of Human Genetics*, *89*(5), 675–681. https://doi.org/10.1016/j.ajhg.2011.10.008

Corces, M. R., Trevino, A. E., Hamilton, E. G., Greenside, P. G., Sinnott-Armstrong, N. A., Vesuna, S., Satpathy, A. T., Rubin, A. J., Montine, K. S., Wu, B., Kathiria, A., Cho, S. W., Mumbach, M. R., Carter, A. C., Kasowski, M., Orloff, L. A., Risca, V. I., Kundaje, A., Khavari, P. A., … Chang, H. Y. (2017). An improved ATAC-seq protocol reduces background and enables interrogation of frozen tissues. *Nature Methods*, *14*(10), 959–962. https://doi.org/10.1038/nmeth.4396

Cormier-Daire, V., Chauvet, M. L., Lyonnet, S., Briard, M. L., Munnich, A., & Le Merrer, M. (2000). Genitopatellar syndrome: A new condition comprising absent patellae, scrotal hypoplasia, renal anomalies, facial dysmorphism, and mental retardation. *Journal of Medical Genetics*, *37*(7), 520–524. https://doi.org/10.1136/jmg.37.7.520

Dobin, A., Davis, C. A., Schlesinger, F., Drenkow, J., Zaleski, C., Jha, S., Batut, P., Chaisson, M., & Gingeras, T. R. (2013). STAR: Ultrafast universal RNA-seq aligner. *Bioinformatics*, *29*(1), 15–21. https://doi.org/10.1093/bioinformatics/bts635

Findlay, G. M., Daza, R. M., Martin, B., Zhang, M. D., Leith, A. P., Gasperini, M., Janizek, J. D., Huang, X., Starita, L. M., & Shendure, J. (2018). Accurate classification of BRCA1 variants with saturation genome editing. *Nature*, *562*(7726), 217–222. https://doi.org/10.1038/s41586-018-0461-z

Gannon, T., Perveen, R., Schlecht, H., Ramsden, S., Anderson, B., Kerr, B., Day, R., Banka, S., Suri, M., Berland, S., Gabbett, M., Ma, A., Lyonnet, S., Cormier-Daire, V., Yilmaz, R., Borck, G., Wieczorek, D., Anderlid, B.-M., Smithson, S., … Clayton-Smith, J. (2015). Further delineation of the KAT6B molecular and phenotypic spectrum. *European Journal of Human Genetics: EJHG*, *23*(9), 1165–1170. https://doi.org/10.1038/ejhg.2014.248

Gaspar, J. M. (2018). NGmerge: Merging paired-end reads via novel empirically-derived models of sequencing errors. *BMC Bioinformatics*, *19*(1), 536. https://doi.org/10.1186/s12859-018-2579-2

Gaspar, J.M. (2018). Genrich: Detecting sites of genomic enrichment. Github. Accessed May 19, 2021. https://github.com/jsh58/Genrich

Goudie, D. R., D'Alessandro, M., Merriman, B., Lee, H., Szeverényi, I., Avery, S., O'Connor, B. D., Nelson, S. F., Coats, S. E., Stewart, A., Christie, L., Pichert, G., Friedel, J., Hayes, I., Burrows, N., Whittaker, S., Gerdes, A.-M., Broesby-Olsen, S., Ferguson-Smith, M. A., … Lane, E. B. (2011). Multiple self-healing squamous epithelioma is caused by a disease-specific spectrum of mutations in TGFBR1. *Nature Genetics*, *43*(4), 365–369. https://doi.org/10.1038/ng.780

Hornbeck, P. V., Zhang, B., Murray, B., Kornhauser, J. M., Latham, V., & Skrzypek, E. (2015). PhosphoSitePlus, 2014: Mutations, PTMs and recalibrations. *Nucleic Acids Research*, *43*(Database issue), D512–D520.

Klein, B. J., Jang, S. M., Lachance, C., Mi, W., Lyu, J., Sakuraba, S., Krajewski, K., Wang, W. W., Sidoli, S., Liu, J., Zhang, Y. I., Wang, X., Warfield, B. M., Kueh, A. J., Voss, A. K., Thomas, T., Garcia, B. A., Liu, W. R., Strahl, B. D., … Kutateladze, T. G. (2019). Histone H3K23-specific acetylation by MORF is coupled to H3K14 acylation. *Nature Communications*, *10*(1), 4724. https://doi.org/10.1038/s41467-019-12551-5

Kolde, R. (2015). Pheatmap: Pretty Heatmaps. R Package Version 1.0. 8. Available.

Kotler, E., Shani, O., Goldfeld, G., Lotan-Pompan, M., Tarcic, O., Gershoni, A., Hopf, T. A., Marks, D. S., Oren, M., & Segal, E. (2018). A systematic p53 mutation library links differential functional impact to cancer mutation pattern and evolutionary conservation. *Molecular Cell*, *71*(1), 178–90.e8. https://doi.org/10.1016/j.molcel.2018.06.012

Langmead, B., & Salzberg, S. L. (2012). Fast gapped-read alignment with Bowtie 2. *Nature Methods*, *9*(4), 357–359. https://doi.org/10.1038/nmeth.1923

Lonardo, F., Lonardo, M. S., Acquaviva, F., Della Monica, M., Scarano, F., & Scarano, G. (2019). Say-Barber-Biesecker-Young-Simpson syndrome and Genitopatellar syndrome: Lumping or splitting? *Clinical Genetics*, *95*(2), 253–261. https://doi.org/10.1111/cge.13127

Love, M. I., Huber, W., & Anders, S. (2014). Moderated estimation of fold change and dispersion for RNA-seq data with DESeq2. *Genome Biology*, *15*(12), 550. https://doi.org/10.1186/s13059-014-0550-8

Malhis, N., Jones, S. J. M., & Gsponer, J. (2019). Improved measures for evolutionary conservation that exploit taxonomy distances. *Nature Communications*, *10*(1), 1556. https://doi.org/10.1038/s41467-019-09583-2

Marangi, G., Di Giacomo, M. C., Lattante, S., Orteschi, D., Patrizi, S., Doronzio, P. N., Riviello, F. N., Vaisfeld, A., Frangella, S., & Zollino, M. (2018). A novel truncating variant within exon 7 of KAT6B associated with features of both Say–Barber–Biesecker–Young–Simpson syndrome and Genitopatellar syndrome: Further evidence of a continuum in the clinical spectrum of KAT6B-related disorders. *American Journal of Medical Genetics Part A*, *176*(2), 455–459.

Mendell, J. R., Goemans, N., Lowes, L. P., Alfano, L. N., Berry, K., Shao, J., Kaye, E. M., & Mercuri, E.; Eteplirsen Study, Group, and Telethon Foundation, D. M. D. Italian Network. (2016). Longitudinal effect of eteplirsen versus historical control on ambulation in duchenne muscular dystrophy. *Annals of Neurology*, *79*(2), 257–271. https://doi.org/10.1002/ana.24555

Mészáros, B., Erdos, G., & Dosztányi, Z. (2018). IUPred2A: Context-dependent prediction of protein disorder as a function of redox state and protein binding. *Nucleic Acids Research*, *46*(W1), W329–W337. https://doi.org/10.1093/nar/gky384

Miller, J., & Humer, C. (2019). Novartis $2 million gene therapy for rare disorder is world's most expensive drug. *Reuters*. https://www.reuters.com/article/us-novartis-genetherapy-idUSKCN1SU1ZP

Niida, Y. O., Mitani, Y., Kuroda, M., Yokoi, A., Nakagawa, H., & Kato, A. (2017). A Say-Barber-Biesecker-Young-Simpson variant of Ohdo syndrome with a KAT6B 10-base pair palindromic duplication: A recurrent mutation causing a severe phenotype mixed with genitopatellar syndrome. *Congenital Anomalies*, *57*(3), 86–88.

Ohdo, S., Madokoro, H., Sonoda, T., & Hayakawa, K. (1986). Mental retardation associated with congenital heart disease, blepharophimosis, blepharoptosis, and hypoplastic teeth. *Journal of Medical Genetics*, *23*(3), 242–244. https://doi.org/10.1136/jmg.23.3.242

Pelletier, N., Champagne, N., Stifani, S., & Yang, X.-J. (2002). MOZ and MORF histone acetyltransferases interact with the runt-domain transcription factor Runx2. *Oncogene*, *21*(17), 2729–2740. https://doi.org/10.1038/sj.onc.1205367

Penttinen, M., Koillinen, H., Niinikoski, H., Mäkitie, O., & Hietala, M. (2009). Genitopatellar syndrome in an adolescent female with severe osteoporosis and endocrine abnormalities. *American Journal of Medical Genetics Part A*, *149A*(3), 451–455. https://doi.org/10.1002/ajmg.a.32644

Posey, J. E., Harel, T., Liu, P., Rosenfeld, J. A., James, R. A., Coban Akdemir, Z. H., Walkiewicz, M., Bi, W., Xiao, R., Ding, Y., Xia, F., Beaudet, A. L., Muzny, D. M., Gibbs, R. A., Boerwinkle, E., Eng, C. M., Sutton, V. R., Shaw, C. A., Plon, S. E., ... Lupski, J. R. (2017). Resolution of disease phenotypes resulting from multilocus genomic variation. *The New England Journal of Medicine*, *376*(1), 21–31. https://doi.org/10.1056/NEJMoa1516767

Rigden, D. J., & Fernández, X. M. (2019). The 26th annual nucleic acids research database issue and molecular biology database collection. *Nucleic Acids Research*, *47*(D1), D1–D7. https://doi.org/10.1093/nar/gky1267

Sapountzi, V., & Cote, J. (2011). MYST-family histone acetyltransferases: Beyond chromatin. *Cellular and Molecular Life Sciences: CMLS*, *68*(7), 1147–1156. https://doi.org/10.1007/s00018-010-0599-9

Say, B., & Barber, N. (1987). Mental retardation with blepharophimosis. *Journal of Medical Genetics*, *24*(8), 511. https://doi.org/10.1136/jmg.24.8.511-a

Shannon, P., Markiel, A., Ozier, O., Baliga, N. S., Wang, J. T., Ramage, D., Amin, N., Schwikowski, B., & Ideker, T. (2003). Cytoscape: A software environment for integrated models of biomolecular interaction networks. *Genome Research*, *13*(11), 2498–2504. https://doi.org/10.1101/gr.1239303

Shaw, N. D., Brand, H., Kupchinsky, Z. A., Bengani, H., Plummer, L., Jones, T. I., Erdin, S., Williamson, K. A., Rainger, J., Stortchevoi, A., Samocha, K., Currall, B. B., Dunican, D. S., Collins, R. L., Willer, J. R., Lek, A., Lek, M., Nassan, M., Pereira, S., ... Talkowski, M. E. (2017). SMCHD1 mutations associated with a rare muscular dystrophy can also cause isolated arhinia and bosma arhinia microphthalmia syndrome. *Nature Genetics*, *49*(2), 238–248. https://doi.org/10.1038/ng.3743

Sheikh, B. N., Dixon, M. P., Thomas, T., & Voss, A. K. (2012). Querkopf is a key marker of self-renewal and multipotency of adult neural stem cells. *Journal of Cell Science*, *125*(Pt 2), 295–309. https://doi.org/10.1242/jcs.077271

Simillion, C., Liechti, R., Lischer, H. E. L., Ioannidis, V., & Bruggmann, R. (2017). Avoiding the pitfalls of gene set enrichment analysis with SetRank. *BMC Bioinformatics*, *18*(1), 151. https://doi.org/10.1186/s12859-017-1571-6

Simpson, M. A., Deshpande, C., Dafou, D., Vissers, L. E. L. M., Woollard, W. J., Holder, S. E., Gillessen-Kaesbach, G., Derks, R., White, S. M., Cohen-Snuijf, R., Kant, S. G., Hoefsloot, L. H., Reardon, W., Brunner, H. G., Bongers, E. M. H. F., & Trembath, R. C. (2012). De novo mutations of the gene encoding the histone acetyltransferase KAT6B cause genitopatellar syndrome. *American Journal of Human Genetics*, *90*(2), 290–294. https://doi.org/10.1016/j.ajhg.2011.11.024

Stark, R., & Brown, G. (2011). DiffBind: Differential binding analysis of ChIP-Seq peak data. *R Package Version*, *100*(4.3), 1–40. https://bioconductor.statistik.tu-dortmund.de/packages/2.13/bioc/vignettes/DiffBind/inst/doc/DiffBind.pdf

Szakszon, K., Berényi, E., Jakab, A., Bessenyei, B., Balogh, E., Köbling, T., Szilvássy, J., Knegt, A. C., & Oláh, E. (2011). Blepharophimosis mental retardation syndrome Say-Barber/Biesecker/Young-Simpson type – New findings with neuroimaging. *American Journal of Medical Genetics. Part A*, *155A*(3), 634–637. https://doi.org/10.1002/ajmg.a.33837

Szakszon, K., Salpietro, C., Kakar, N., Knegt, A. C., Olah, E., Dallapiccola, B., & Borck, G. (2013). De novo mutations of the gene encoding the histone acetyltransferase KAT6B in two patients with Say-Barber/Biesecker/Young-Simpson syndrome. *American Journal of Medical Genetics Part A*, *161A*(4), 884–888. https://doi.org/10.1002/ajmg.a.35848

Vlckova, M., Simandlova, M., Zimmermann, P., Stranecky, V., Hartmannova, H., Hodanova, K., Havlovicova, M., Hancarova, M., Kmoch, S., & Sedlacek, Z. (2015). A patient showing features of both SBBYSS and GPS supports the concept of a KAT6B-related disease spectrum, with mutations in mid-exon 18 possibly leading

to combined phenotypes. *European Journal of Medical Genetics*, *58*(10), 550–555. https://doi.org/10.1016/j.ejmg.2015.09.004

Voss, A. K., Collin, C., Dixon, M. P., & Thomas, T. (2009). Moz and retinoic acid coordinately regulate H3K9 acetylation, hox gene expression, and segment identity. *Developmental Cell*, *17*(5), 674–686. https://doi.org/10.1016/j.devcel.2009.10.006

Wainwright, C. E., Elborn, J. S., Ramsey, B. W., Marigowda, G., Huang, X., Cipolli, M., Colombo, C., Davies, J. C., De Boeck, K., Flume, P. A., & Konstan, M. W. (2015). Lumacaftor-ivacaftor in patients with cystic fibrosis homozygous for Phe508del CFTR. *The New England Journal of Medicine*, *373*(3), 220–231.

Walsh, I., Martin, A. J. M., Di Domenico, T., & Tosatto, S. C. E. (2012). ESpritz: Accurate and fast prediction of protein disorder. *Bioinformatics*, *28*(4), 503–509. https://doi.org/10.1093/bioinformatics/btr682

Yu, G., Wang, L.-G., Han, Y., & He, Q.-Y. (2012). clusterProfiler: An R package for comparing biological themes among gene clusters. *OMICS: A Journal of Integrative Biology*, *16*(5), 284–287. https://doi.org/10.1089/omi.2011.0118

Yu, G., Wang, L.-G., & He, Q.-Y. (2015). ChIPseeker: An R/bioconductor package for ChIP peak annotation, comparison and visualization. *Bioinformatics*, *31*(14), 2382–2383. https://doi.org/10.1093/bioinformatics/btv145

Zhang, L. X., Lemire, G., Gonzaga-Jauregui, C., Molidperee, S., Galaz-Montoya, C., Liu, D. S., Verloes, A., Shillington, A. G., Izumi, K., Ritter, A. L., Keena, B., Zackai, E., Li, D., Bhoj, E., Tarpinian, J. M., Bedoukian, E., Kukolich, M. K., Innes, A. M., Ediae, G. U., ... Campeau, P. M. (2020). Further delineation of the clinical spectrum of KAT6B disorders and allelic series of pathogenic variants. *Genetics in Medicine*, *22*(8), 1338–1347. https://doi.org/10.1038/s41436-020-0811-8

Zhu, L., Lv, L., Dingwen, W. U., & Shao, J. (2020). KAT6B genetic variant identified in a short stature Chinese infant: A report of physical growth in clinical spectrum of KAT6B-related disorders. *Frontiers in Pediatrics*, *8*(April), 124. https://doi.org/10.3389/fped.2020.00124

WEB RESOURCES

UniProt. http://www.uniprot.org/

SUPPORTING INFORMATION

Additional Supporting Information may be found online in the Supporting Information section.

How to cite this article: Yabumoto, M., Kianmahd, J., Singh, M., Palafox, M. F., Wei, A., Elliott, K., Goodloe, D. H., Dean, S. J., Gooch, C., Murray, B. K., Swartz, E., Schrier Vergano, S. A., Towne, M. C., Nugent, K., Roeder, E. R., Kresge, C., Pletcher, B. A., Grand, K., Graham, J. M. Jr., ... Arboleda, V. A. (2021). Novel variants in *KAT6B* spectrum of disorders expand our knowledge of clinical manifestations and molecular mechanisms. *Molecular Genetics & Genomic Medicine*, 9, e1809. https://doi.org/10.1002/mgg3.1809